Supplementary Information

Microfluidic Probe for Single-Cell Analysis in Adherent Tissue Culture

Aniruddh Sarkar[1‡], Sarah Kolitz[2‡], Douglas A. Lauffenburger[2], Jongyoon Han[1,2*]

[1]Department of Electrical Engineering and Computer Science,

[2]Department of Biological Engineering

Massachusetts Institute of Technology, Cambridge, MA, USA

Supplementary Figure 1. Repeatability of microfluidic probe device performance parameters

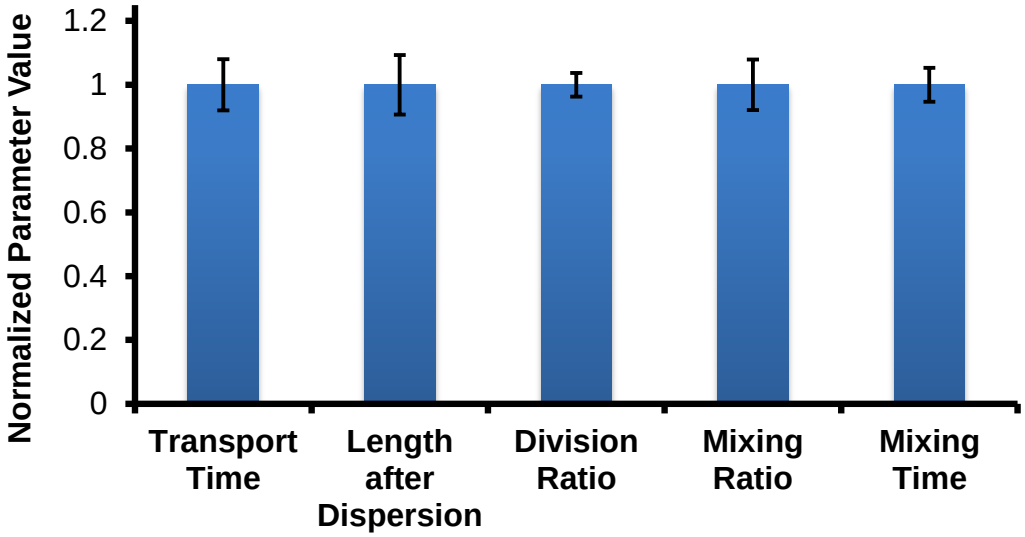

See Supplementary Note 1. All parameter values and errors are normalized to their respective mean value. Error bars represent standard deviations (n > 3 for each).

Supplementary Figure 2. Procedure for lysis quantification.

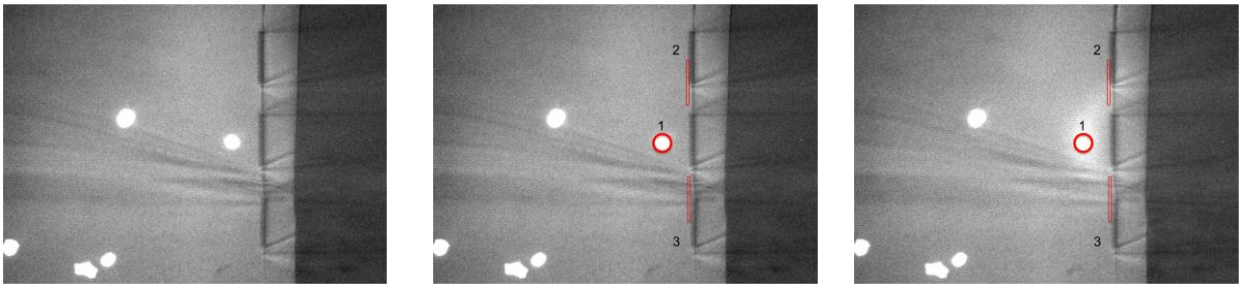

a) See Supplementary Note 2. We used ImageJ to quantify fluorescence from the marked regions across the time course of the lysis procedure (area 1: cell; area 2: upper intake of device; area 3: lower intake of device). Shown here are images captured before lysis (left image; middle image is the same as the left image, with bounding boxes used for quantification shown; t=0) and during lysis (right image; t=11 s).

Area 1. Lysis

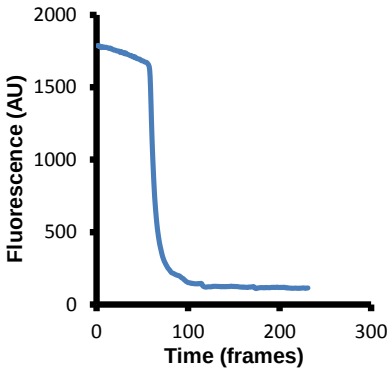

Area 2. Upper device intake

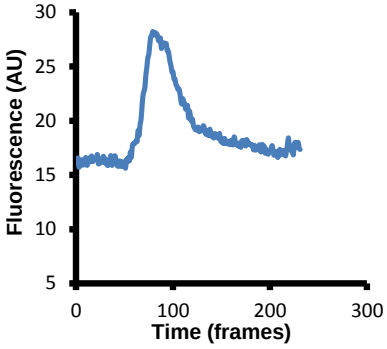

Area 3. Lower device intake

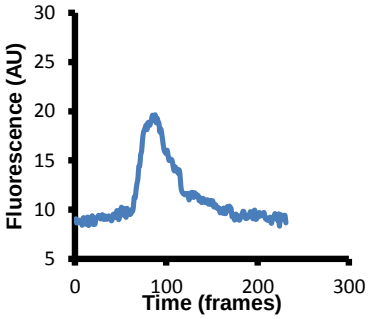

b) Time series values for each box were corrected for background light fluctuations to obtain curves for lysis (area 1) and capture at upper and lower intake (areas 2 and 3). Parameters were extracted from these curves as described in Supplementary Note 2.

Supplementary Figure 3. Correlation of lysis parameters. See Supplementary Note 2.

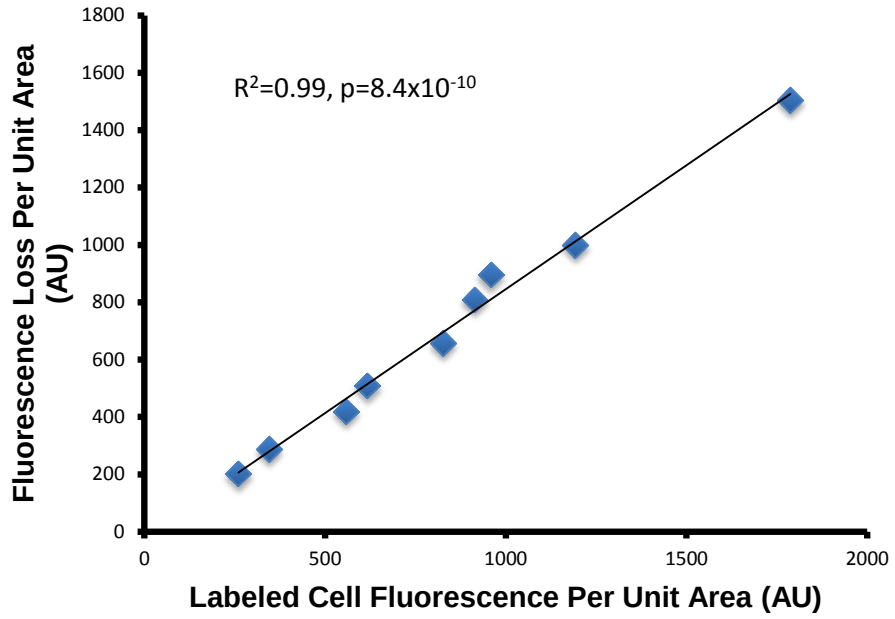

a) Mean fluorescence loss plotted against mean initial fluorescence. A regression line is shown. The Pearson correlation coefficient is 0.99, with p value of 8.4×10^{-10} (calculated using PEARSON and TDIST functions in Excel). Each point represents a single cell.

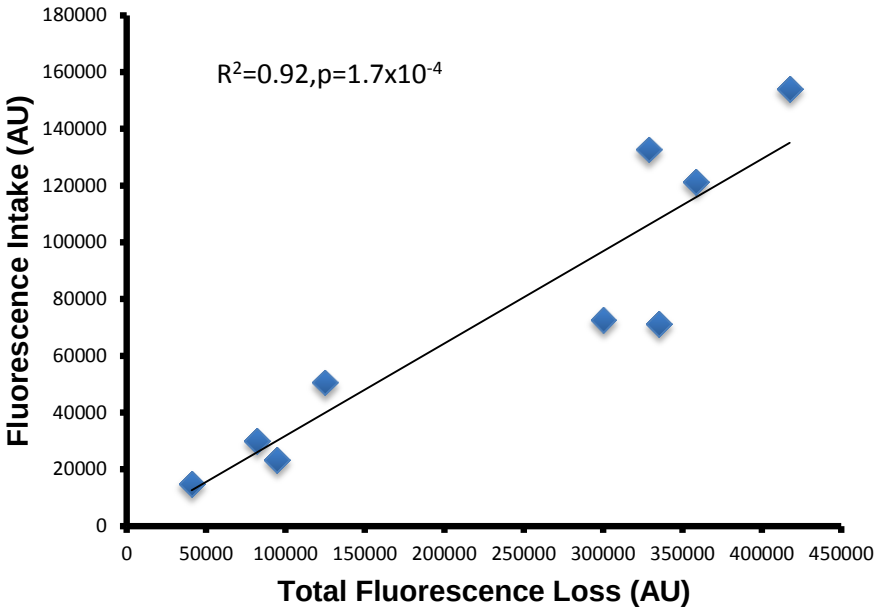

b) Fluorescence intake versus total fluorescence loss. Fluorescence intake correlates with total fluorescence loss. A regression line is shown. The Pearson correlation coefficient is 0.92, with p value of $1.7x10^{-4}$. Each point represents a single cell.

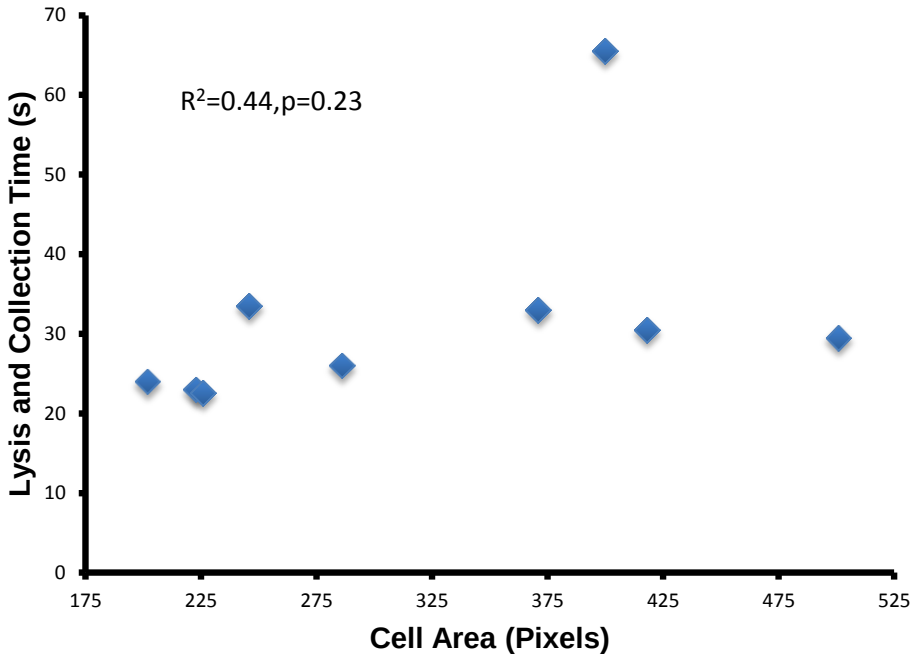

c) Lysis and collection time versus cell area. The lysis and collection time is independent of the area of the cell being lysed. The Pearson correlation coefficient is 0.44, with p value of 0.23.

Supplementary Figure 4. a) Bulk-level Akt activity time-course. b) Single-cell Akt activity time-course.

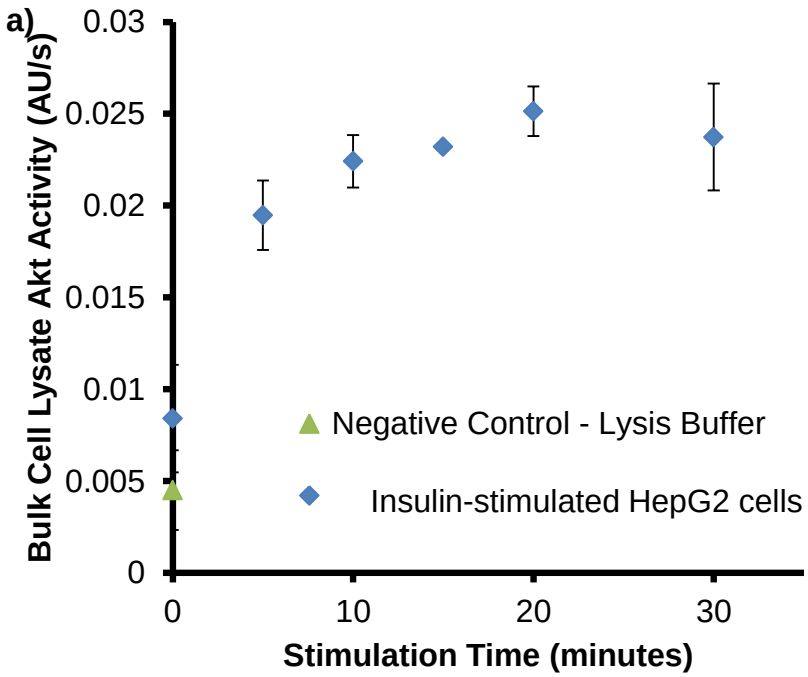

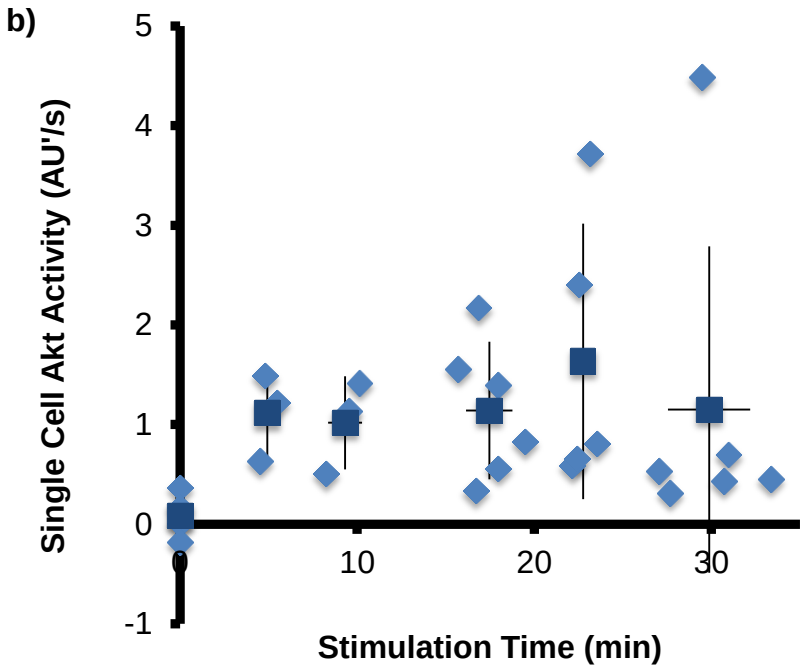

(a) Data obtained at the bulk level for Akt activity time-course under insulin stimulation (n=3). Error bars represent standard deviation. The extent of cell-to-cell variation under these stimulation conditions was unknown a priori. As shown in (b), the single-cell activity measurements present a mean behavior similar to the bulk measurements, while significant variation is seen in the measurements for the individual cells. One contributing factor to this variation could be technical error of the on-device measurement, which we have measured to be 7% for bulk Akt on the device. The single cell measurements, however, show fluctuations beyond what is expected due to this measured technical error, and therefore are likely to reflect biological variation between individual cells that is not visible in the bulk-level assay. True biological differences may also exist due to differences in the single-cell assay conditions versus the bulk assay conditions. Inevitable slight differences in conditions between these assays, resulting from the manner in which they were performed, include the presence of cell culture medium in the reaction on the device. Note that different arbitrary activity units used on the y-axes in (a) and (b) due to different fluorimetric sensitivities of the two assay platforms. Error bars represent standard deviation.

Supplementary Figure 5. Activity of recombinant Akt measured on the plate reader.

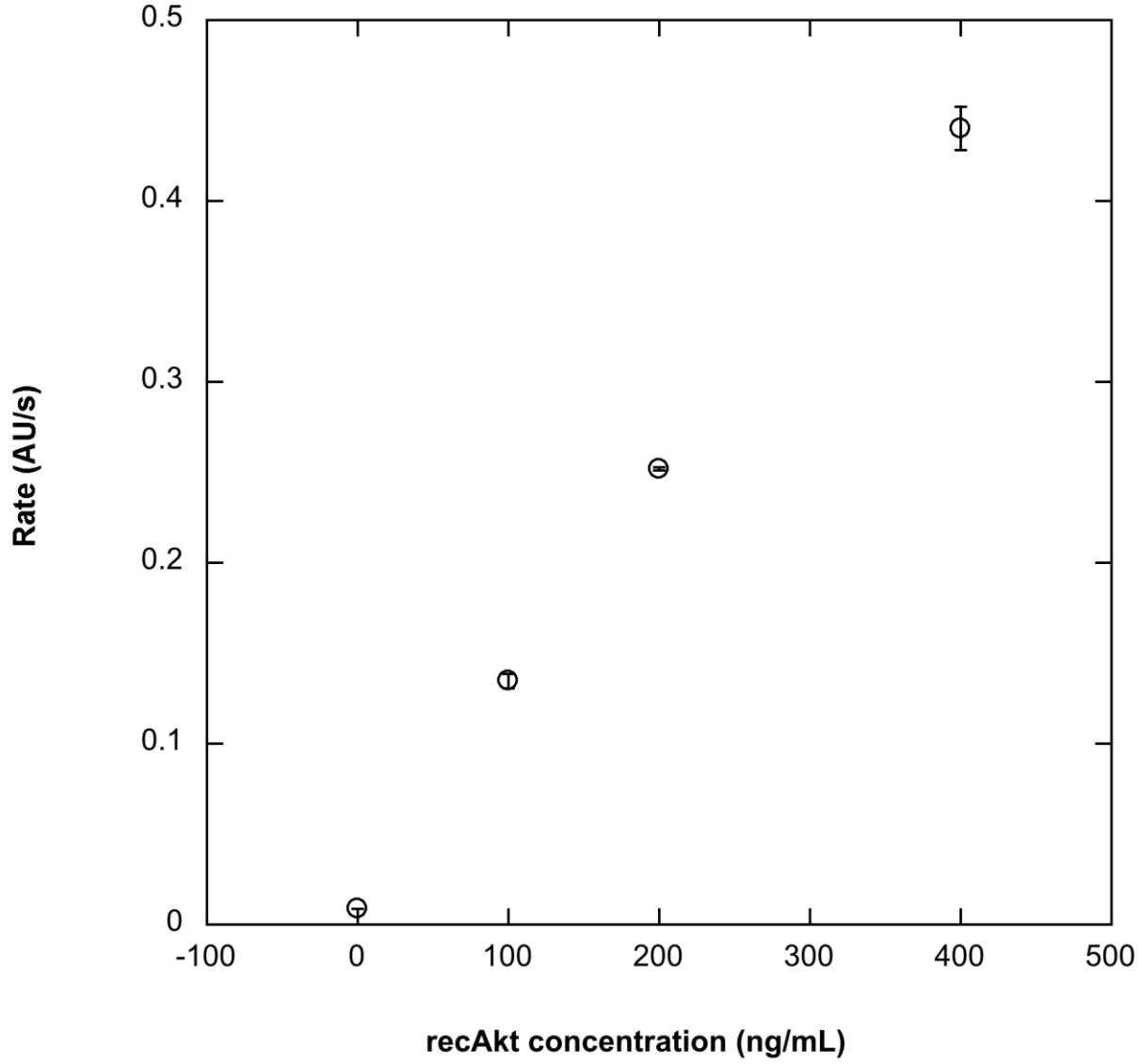

Activity of recombinant Akt measured on the plate reader yields a limit of detection of 0.51 ng.

Error bars represent standard deviation; n=2.

Supplementary Figure 6. Bulk lysate with differing activity levels measured on device.

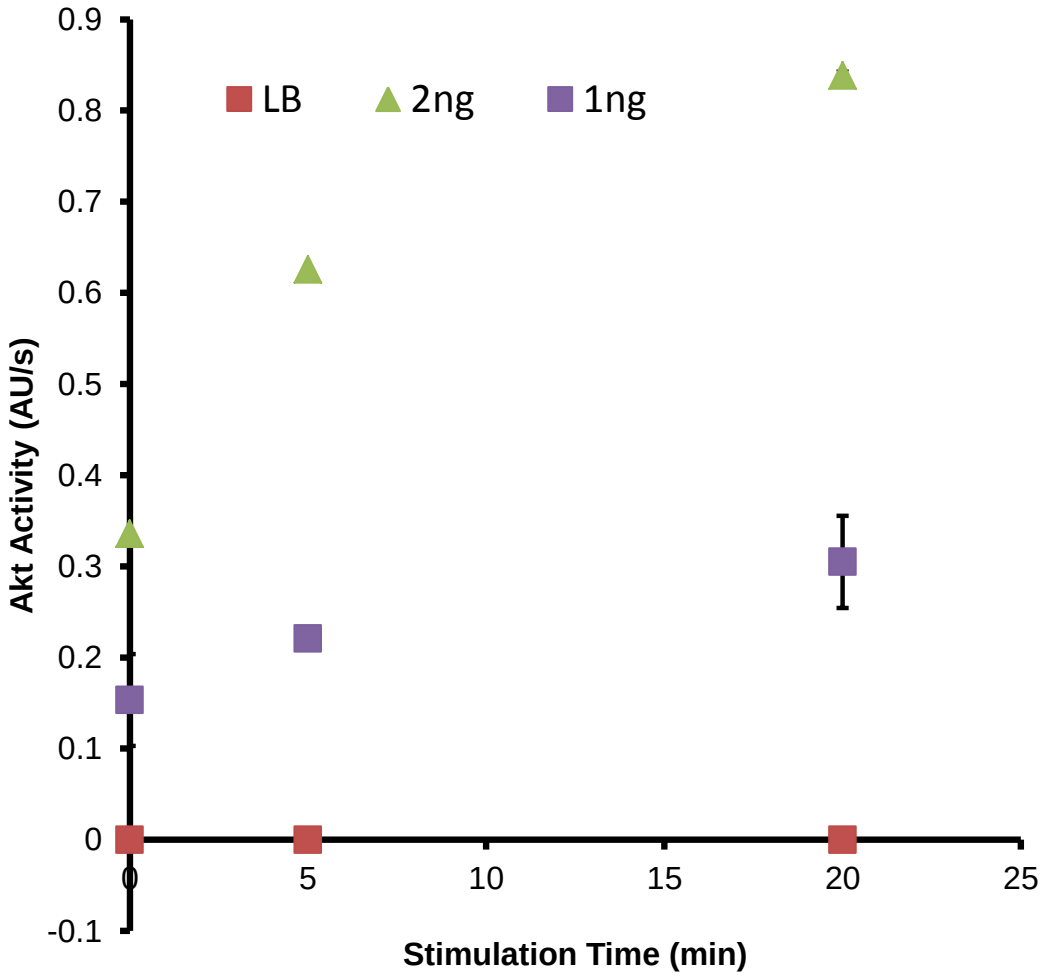

The differing Akt activity levels resulting from different times of stimulation were resolvable on the device. Averages of at least two experiments are shown (for most points, error bars are not visible because they are smaller than the point markers). Error bars represent standard deviation.

Supplementary Figure 7. MK2 activity measured on device from diluted bulk lysate.

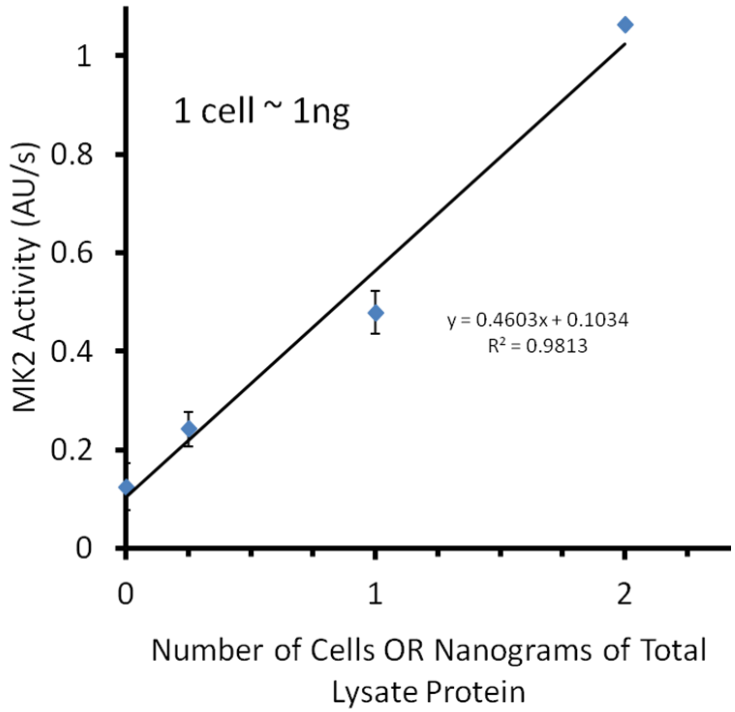

Similar or higher sensitivity to that for Akt is seen in MK2 calibration with bulk-level lysate. Error bars represent standard deviation.

Supplementary Figure 8. Histogram of cell minimum Feret diameter.

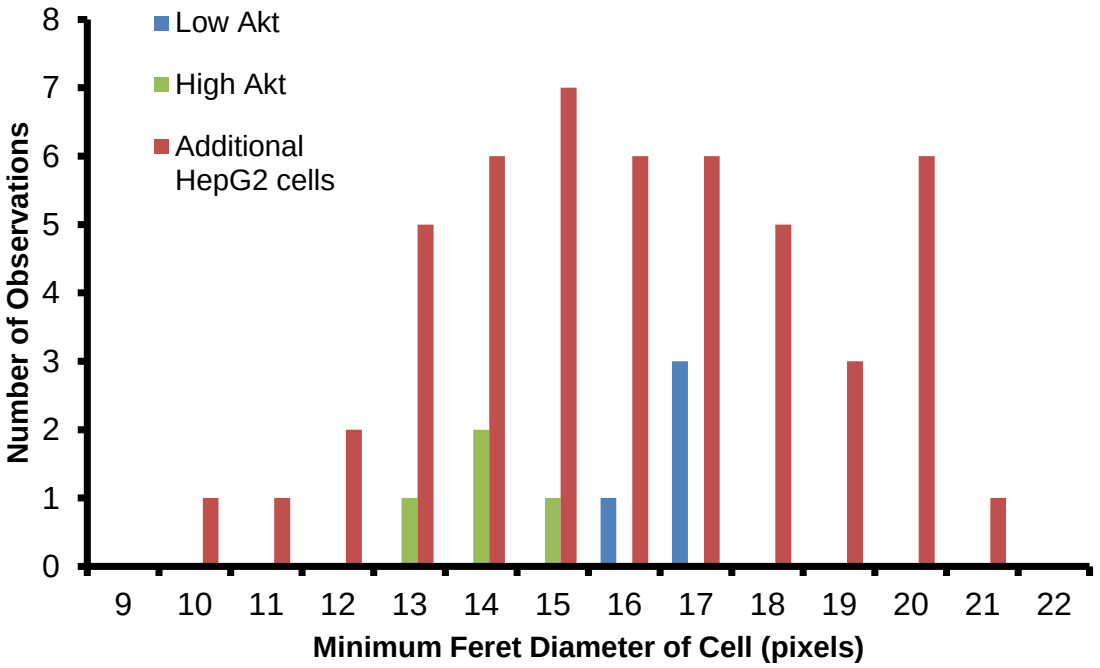

A histogram of measured cell minimum Feret diameter for 49 additional cells (red) out of the HepG2 population as well as cells whose Akt levels were measured using the device (green and blue) is plotted. This demonstrates that the cells with measured Akt values lie within the overall distribution of this morphological parameter, and supports the idea that multiple morphological subtypes could be present in the cell population under these assay conditions.

Supplementary Figure 9. Normalization of Akt data by corresponding GAPDH reading for each cell.

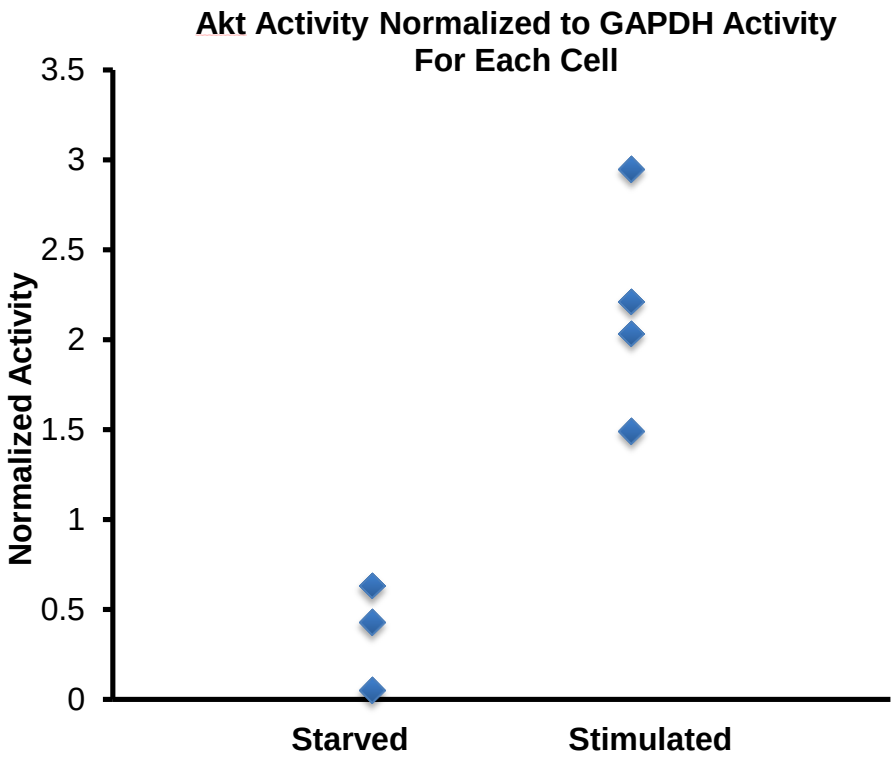

Akt activities normalized by GAPDH activity level on an individual cell basis show a similar pattern of response to insulin stimulation, comparing serum-starved cells with cells that responded to insulin stimulation with an increase in Akt activity ("high Akt" cells).

Supplementary Figure 10. Example distributions.

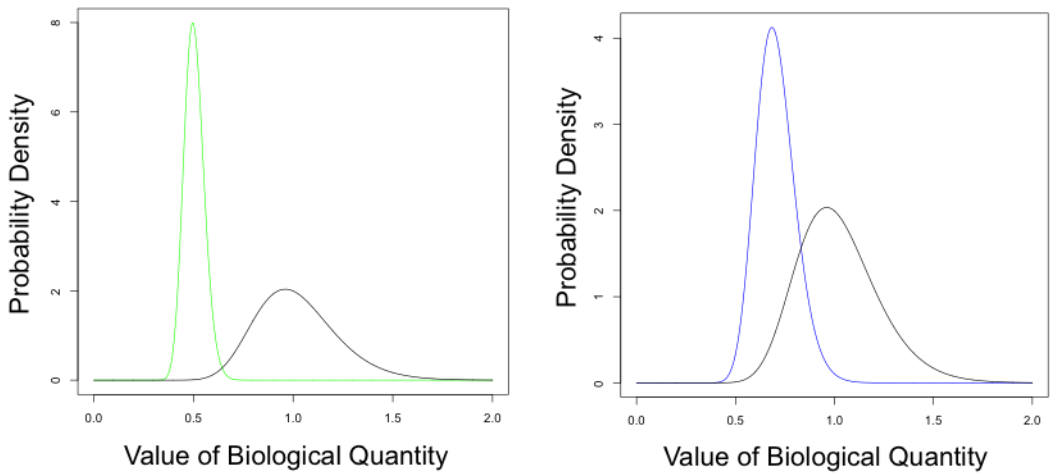

(i)

(ii)

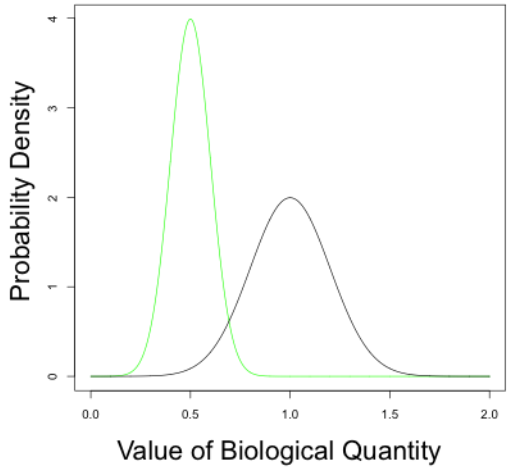

(iii)

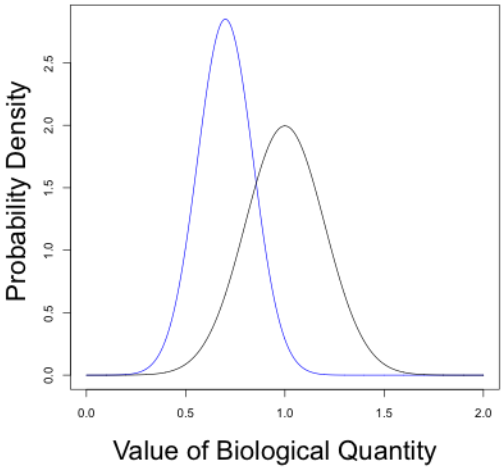

(iv)

See Supplementary Note 3. The value on the x-axis represents the value of the biological quantity (e.g., activity). Two log-normal distributions having differing degrees of overlap are plotted in each of (i) and (ii). Similarly, two normal distributions having differing degrees of overlap are plotted in each of (iii) and (iv). In (i) and (iii), the difference between the means is 0.5 (μ_{lo}=0.5 versus μ_{hi}=1.0), and in (ii) and (iv) the difference is 0.2 (μ_{lo}=0.8 versus μ_{hi}=1.0).

These distributions represent those according to which “true” biological values were generated, assuming a biological CV of 20%.

Supplementary Figure 11. Simulation results for 20% or 30% biological CV and normal or log-normal biological distributions.

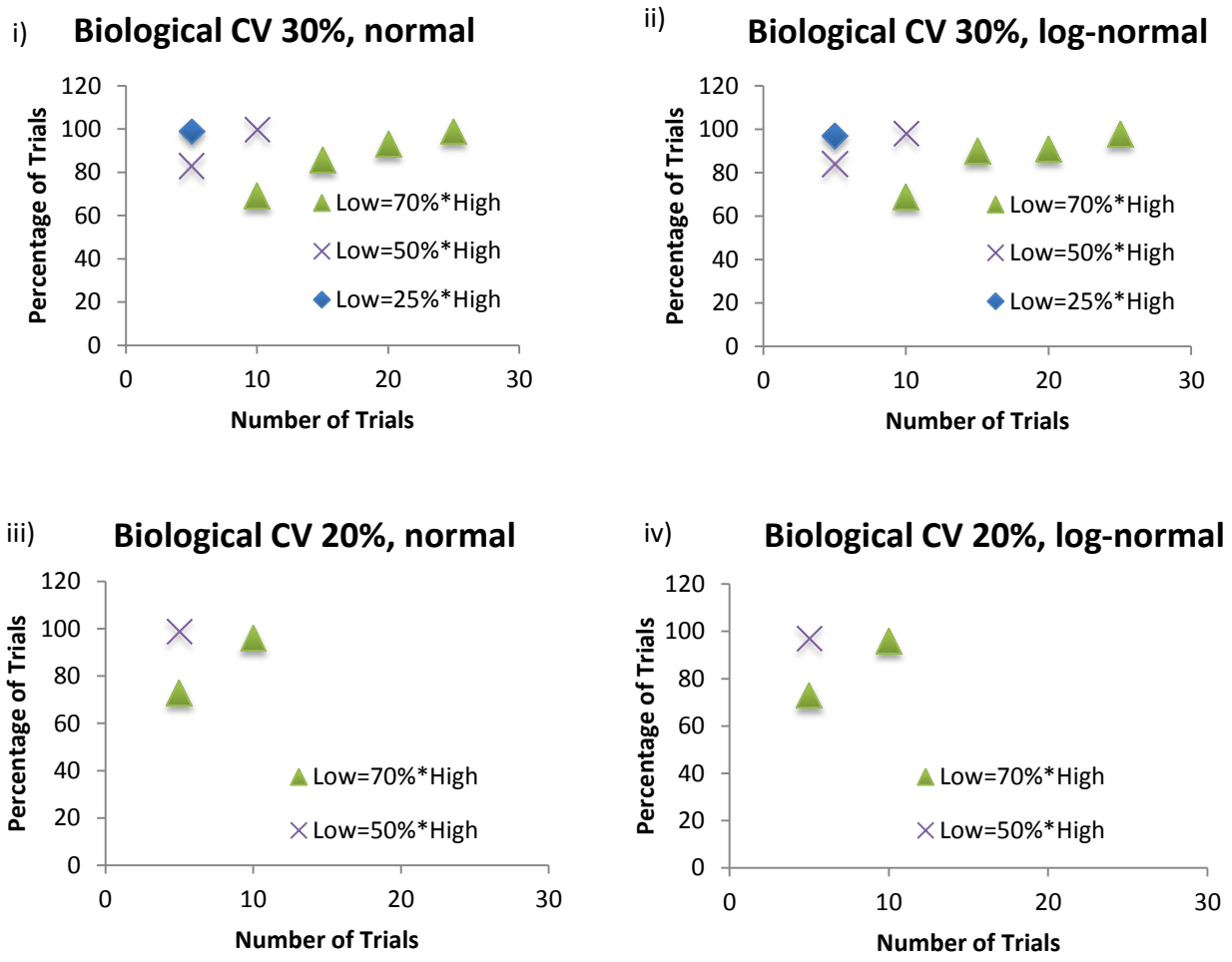

See Supplementary Note 3. In each of (i)-(iv), the percentage of trials in which the two cell populations were statistically distinguishable is plotted against the number of measurements (cells measured) from each population. The "low" mean values shown in the legend correspond to a difference between high and low means of 0.75 (μ_{lo}=0.25 versus μ_{hi}=1.0), 0.5 (μ_{lo}=0.5 versus μ_{hi}=1.0), and 0.3 (μ_{lo}=0.7 versus μ_{hi}=1.0), respectively. In (i) and (ii), results are shown

for a biological CV of 30%, while in (iii) and (iv), results are shown for a biological CV of 20%. Panels (i) and (iii) show results for a biological distribution that is assumed to be normal, and panels (ii) and (iv) show results for a log-normal distribution of biological data.

Supplementary Figure 12. SA-β-gal assay.

a) 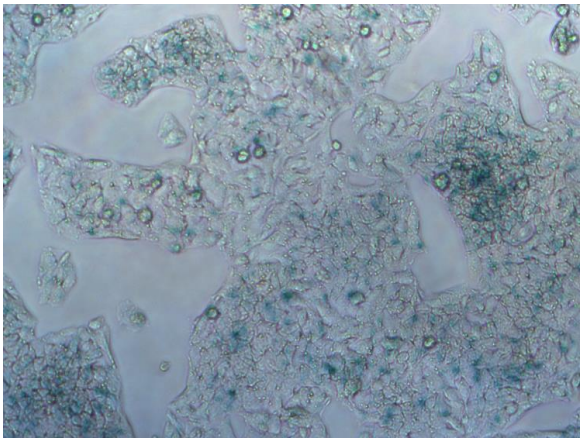 **b)** 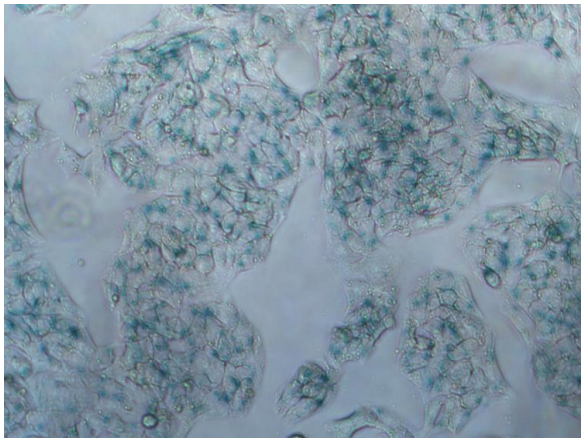

c) 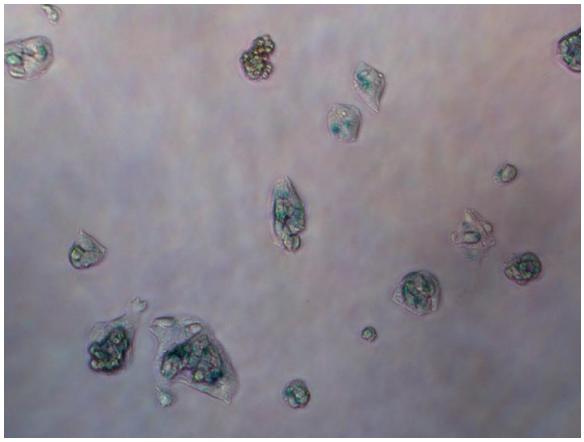

See Supplementary Note 4. Representative phase-contrast images are shown for: (a) Negative control (normal culture conditions); (b) Positive control (70 h doxorubicin treatment); (c) Sparse plating condition. Appearance of blue color indicates presence of senescence-associated beta-galactosidase activity.

Supplementary Tables

Supplementary Table 1. Microfluidic probe device performance parameters

Parameter	Average (n>3)	Standard Deviation
Transport Time	59.5s	4.8s
Length after dispersion (relative to chamber length: 1mm)	0.9	0.1
Division Ratio	1	0.04
Mixing Ratio	4.1	0.3
Mixing Time Constant	1.8min	0.1min

Supplementary Table 2.

a) Simulation results, technical error CV of 10%

Biological CV:	Number of measurements (cells):	Distance between means:	"Low" mean value	"Low" mean value percent of "high" mean:	Percentage of runs where "low" was significantly lower than "high" assuming normal distribution:	Percentage of runs where "low" was significantly lower than "high" assuming log-normal distribution:	# runs:
20%	5	0.5	0.5	50%	99	100	100
20%	5	0.3	0.7	70%	73	77	100
20%	10	0.3	0.7	70%	96	99	100
30%	5	0.75	0.25	25%	99	100	100
30%	5	0.5	0.5	50%	83	94	100
30%	10	0.5	0.5	50%	100	100	100
30%	10	0.3	0.7	70%	69	88	100
30%	15	0.3	0.7	70%	86	96	100
30%	20	0.3	0.7	70%	93	98	100
30%	25	0.3	0.7	70%	99	100	100

b) Simulation results, technical error CV of 20%

Biological CV:	Number of measurements (cells):	Distance between means:	"Low" mean value	"Low" mean value percent of "high" mean:	Percentage of runs where "low" was significantly lower than "high" assuming normal distribution:	Percentage of runs where "low" was significantly lower than "high" assuming log-normal distribution:	# runs:
20%	5	0.5	0.5	50%	99	100	100
20%	5	0.3	0.7	70%	73	77	100
20%	10	0.3	0.7	70%	96	99	100
30%	5	0.75	0.25	25%	99	100	100
30%	5	0.5	0.5	50%	83	94	100
30%	10	0.5	0.5	50%	100	100	100
30%	10	0.3	0.7	70%	69	88	100
30%	15	0.3	0.7	70%	86	96	100
30%	20	0.3	0.7	70%	93	98	100
30%	25	0.3	0.7	70%	99	100	100

Supplementary Table 3. Cell counts for senescence-associated beta-galactosidase (SA-β-gal) assay. See Supplementary Note 4.

	Total # cells counted	% SA-β-gal+ (blue) cells
Positive Control (Dox condition)	1682	64
Negative Control (normal condition)	2737	25
Sparse Condition	517	63

Supplementary Notes

Supplementary Note 1. Microfluidic probe device performance characterization

We evaluated the performance and repeatability of the individual modules of the microfluidic probe: single cell lysis and capture, lysate transport and resultant dispersion, lysate sub-division and mixing with assay buffer. The evaluation of the performance of single cell lysis and capture efficiency is detailed in Supplementary Note 2. All the other modules were tested by imaging the flow of a bolus of a suspension of fluorescently labeled protein (Alexa488-BSA) as a model for the cell lysate. The device was set up as for the single cell assay as described in the Methods section. A bolus of fluorescent protein suspension was released from the lysis buffer output by programming the syringe pump controlling to turn the flow on for a short fixed duration (5s). This bolus was then captured back using the lysate input channels. Lysate transport times (Supplementary Fig. 1) were evaluated by measuring the time taken for the bolus to travel from the tip of the device to the chamber. The length of the bolus after transport to the reaction chamber was used to estimate dispersion during transport. Lysate sub-division ratio was evaluated by measuring the relative fluorescence in the four chambers after sub-division of the bolus, mixing with non-fluorescent assay buffer and capture of the mixture. Mixing ratios were also separately evaluated by comparing the fluorescence in each chambers after capture of the mixture to the fluorescence in the same chamber when it is completely filled with the fluorescent protein suspension. Mixing time was obtained by directly imaging the mixing of the subdivided fluorescent protein bolus with non-fluorescent assay buffer. The results of these experiments are summarized in Supplementary Fig. 1 and Supplementary Table 1.

Supplementary Note 2. Lysis quantification procedure and results

Each cell lysis procedure was imaged. We used these images of lysis of cells labeled with fluorescent Cell Tracker dye to quantify the lysis time and capture efficiency. A representative example is shown in Supplementary Fig. 2.

We defined the start time (t_{start}) of lysis as the time at which the difference between successive data points exceeded 10% of the starting value. To determine the end time (t_{end}) of lysis, for each point we calculated the average of that point with the four preceding values, and the average of the differences between those points, then took the ratio. We set t_{end} as the time at which the ratio of the average local differences to the average local values fell to below 10%. (We used this window approach to allow t_{end} to be determined by the overall local shape of the curve rather than by noisy fluctuations.) The lysis and capture time was determined by taking the difference between t_{end} and t_{start}. The mean fluorescence loss (per unit area) was determined as the difference in fluorescence between t_{end} and t_{start}. The total fluorescence lost from the cell was determined by multiplying the mean fluorescence loss (or average fluorescence loss per unit area) by the cell area. Mean fluorescence intensities and areas were quantified using ImageJ.

We integrated the area underneath each intake peak by finding the average value and multiplying this by the width of the peak. We added the two intake values together and multiplied by the size of the quantification area to obtain the total fluorescence intake. Note that this quantity is not expected to equal the total starting fluorescence value observed for the intact cell, as differences in height as well as location in the microscope field will affect the fluorescence intensity observed. We find, however, that the total fluorescence intake correlates with the total starting fluorescence (Supplementary Fig. 3), indicating that the amount captured consistently corresponds to the amount present in the cell before lysis.

Supplementary Note 3. Simulation method

These simulations were conducted using the statistical software package R. We posited a scenario in which two biological populations exist with respect to a particular activity, a "high" and a "low" population. We assumed that for each of these populations, around the mean "high" or "low" value (μ_{hi}, μ_{lo}) would be a range of biological values distributed normally or log-normally with some coefficient of variation (CV). A log-normal distribution with CV 15-30% has been observed for protein and mRNA levels in mammalian cells.[3, 32, 34] For several different values of biological CV, we chose a fixed "high" mean, and varied the "low" mean value to bring the "high" and "low" distributions to varying degrees of overlap. (For example, Supplementary Fig. 10.) Using these parameters we generated "true" biological values.

Subsequent to generating these "true" values, we then generated "measured" values incorporating the measured technical error of the measurement. For each "true" data point a "measured" point was generated from a normal distribution centered around the "true" value with the measured technical CV (7% for Akt; we used 10% in our calculations to be conservative). We then tested whether the two populations were statistically distinguishable on the basis of these "measured" points, using the Student's t-test. We generated many realizations of such scenarios (100 runs per condition) and observed the percentage of runs in which the two populations were statistically significantly distinguishable using the Student's t-test. As shown in Supplementary Table 2, assuming a 20% biological variation, the two populations of cells could be distinguished in >90% of trials with as few as five or ten cells measured per population, depending on the extent of the difference between low and high means. For a biological CV of 30%, two populations whose means differed by only 30% could be distinguished in at least 90% of trials with 20 cell measurements from each population assuming a normal distribution of

biological data, and this number fell to 15 cell measurements from each population when a log-normal distribution was assumed (Supplementary Fig. 11).

Note that these simulations assume a division of cells into two groups of interest, and address the number of measurements needed to identify a difference in a biochemical measurement between these groups of cells. This represents a valuable use case for this device. For example, beginning with an observed phenotypic heterogeneity among cells, indicated by the variation in some marker (e.g. fluorescent), morphological characteristic or even a heterogeneous behavior (e.g. speed of migration), the single cell assay technique can be used to investigate whether there exists an underlying signaling (or indeed other biochemical) heterogeneity associated with the heterogeneous behavior/phenotype. The existence of phenotypic heterogeneity would thus provide an a priori basis of subsets of cells to investigate.

Supplementary Note 4. Senescence-associated beta-galactosidase (SA-β-gal) assay

A senescence-associated beta-galactosidase (SA-β-gal) assay revealed increased SA-β-gal activity under the conditions of the single-cell assay (sparsely plated at 5000-10,000 cells/cm^2; 63% cells showed staining) relative to control (higher density of 100,000 cells/cm^2; 25% cells showed staining), to the same level as a positive control (doxorubicin treatment; 64% cells showed staining) (Supplementary Table 3). A detailed mapping of cell morphological parameters to SA-β-gal staining, however, was made challenging by the fact that the percentage of single HepG2 cells (whose morphology is the most relevant for comparison as well as easiest to measure) exhibiting SA-β-gal staining is high and thus resolving morphological differences that

correlate with this staining is as yet challenging. A different assay for senescence may be needed for connecting morphology and Akt activity level with senescence in HepG2 cells.

Supplementary Methods.

Senescence-associated beta-galactosidase staining method

Senescence-associated beta-galactosidase assays were conducted using Sigma kit CS-0030. Briefly, cells were fixed, then stained with staining mixture for 3 h at 37 °C and atmospheric CO_2. Cells were then stained using Hoechst for identification of cell nuclei and imaged using phase-contrast and DAPI to observe SA-β-gal and Hoechst staining, respectively. Total number of cells was quantified in ImageJ by grayscale-converting and thresholding Hoechst images, applying the Watershed algorithm to help subdivide clumped particles, then using the ImageJ Analyze Particles function. The number of blue cells was counted using the ImageJ Cell Counter plugin. The percentage of cells exhibiting a blue color was calculated. HepG2 cells were cultured and plated as described in the main text, either under the conditions of the single-cell assay (sparsely plated at 5000-10,000 cells/cm^2), or negative control conditions (higher density of 100,000 cells/cm^2). As a positive control, cells were treated with 50 ng/mL doxorubicin for 70 hours. [43]

Supplementary Reference

43. Kim TR, Lee HM, Lee SY, Kim EJ, Kim KC, Paik SG, *et al.* SM22alpha-induced activation of p16INK4a/retinoblastoma pathway promotes cellular senescence caused by a subclinical dose of gamma-radiation and doxorubicin in HepG2 cells. *Biochem Biophys Res Commun* 2010, 400(1): 100-105.